

## Excited Baryons in Lattice QCD

W. Melnitchouk<sup>1,2</sup>, S. Bilson-Thompson<sup>1</sup>, F.D.R. Bonnet<sup>1</sup>, F.X. Lee<sup>2,3</sup>, D.B. Leinweber<sup>1</sup>,  
A.G. Williams<sup>1</sup>, J.M. Zanotti<sup>1</sup> and J.B. Zhang<sup>1</sup>

<sup>1</sup> *Department of Physics and Mathematical Physics and  
Special Research Centre for the Subatomic Structure of Matter,  
University of Adelaide, 5005, Australia*

<sup>2</sup> *Jefferson Lab, 12000 Jefferson Avenue, Newport News, VA 23606*

<sup>3</sup> *Center for Nuclear Studies, Department of Physics,  
The George Washington University, Washington, D.C. 20052*

### Abstract

We present first results of calculations of masses of positive and negative parity excited baryons in lattice QCD using an  $\mathcal{O}(a^2)$  improved gluon action and a fat-link clover fermion action in which only the irrelevant operators are constructed with fat links. The results are in agreement with earlier calculations of  $N^*$  resonances using improved actions and exhibit a clear mass splitting between the nucleon and its chiral partner. The results also indicate a splitting between the lowest  $J^P = \frac{1}{2}^-$  states for the two standard nucleon interpolating fields. The study of different  $\Lambda$  interpolating fields suggests a similar splitting between the lowest two  $\Lambda^{1/2^-}$  octet states. However, the empirical mass suppression of the  $\Lambda^*(1405)$  is not evident in these quenched QCD simulations, suggesting an important role for the meson cloud of the  $\Lambda^*(1405)$  or a need for more exotic interpolating fields.

PACS number(s): 11.15.Ha, 12.38.Gc, 12.38.Aw

## I. INTRODUCTION

Understanding the dynamics responsible for baryon excitations provides valuable insight into the forces which confine quarks inside baryons and into the nature of QCD in the nonperturbative regime. This is a driving force behind the experimental effort of the CLAS Collaboration at Jefferson Lab, which is currently accumulating data of unprecedented quality and quantity on various  $N \rightarrow N^*$  transitions. With the increased precision of the data comes a growing need to understand the observed  $N^*$  spectrum within QCD. Although phenomenological low-energy models of QCD have been successful in describing many features of the  $N^*$  spectrum (for a recent review see Ref. [1]), they leave many questions unanswered, and calculations of  $N^*$  properties from first principles are indispensable.

One of the long-standing puzzles in spectroscopy has been the low mass of the first positive parity excitation of the nucleon (the  $J^P = \frac{1}{2}^+$   $N^*(1440)$  Roper resonance) compared with the lowest lying odd parity excitation. In a valence quark model, in a harmonic oscillator basis, the  $\frac{1}{2}^-$  state naturally occurs below the  $N = 2, \frac{1}{2}^+$  state [2]. Without fine tuning of parameters, valence quark models tend to leave the mass of the Roper resonance too high. Similar difficulties in the level orderings appear for the  $\frac{3}{2}^+$   $\Delta^*(1600)$  and  $\frac{1}{2}^+$   $\Sigma^*(1690)$ , which has led to speculations that the Roper resonances may be more appropriately viewed as “breathing modes” of the confining cavity [3], or described in terms of meson-baryon dynamics alone [4], or as hybrid baryon states with explicitly excited glue field configurations [5].

Another challenge for spectroscopy is presented by the  $\Lambda^{1/2-}(1405)$ , whose anomalously small mass has been interpreted as an indication of strong coupled channel effects involving  $\Sigma\pi$ ,  $\bar{K}N$ ,  $\dots$  [6], and a weak overlap with a three-valence constituent-quark state. In fact, the role played by Goldstone bosons in baryon spectroscopy has received considerable attention recently [7,8].

It has been argued [9] that a spin-flavor interaction associated with the exchange of a pseudoscalar nonet of Goldstone bosons between quarks can better explain the level orderings and hyperfine mass splittings than the traditional (color-magnetic) one gluon exchange mechanism. On the other hand, some elements of this approach, such as the generalization to the meson sector or consistency with the chiral properties of QCD, remain controversial [1,10,11]. Furthermore, neither spin-flavor nor color-magnetic interactions are able to account for the mass splitting between the  $\Lambda^{1/2-}(1405)$  and the  $\Lambda^{3/2-}(1520)$  (a splitting between these can arise in constituent quark models with a spin-orbit interaction, however, this is known to lead to spurious mass splittings elsewhere [1,12]). Recent work [13] on negative parity baryon spectroscopy in the large- $N_c$  limit has identified important operators associated with spin-spin, spin-flavor and other interactions which go beyond the simple constituent quark model, as anticipated by early QCD sum-rule analyses [14].

The large number of states predicted by the constituent quark model and its generalizations which have not been observed (the so-called “missing” resonances) presents another problem for spectroscopy. If these states do not exist, this may suggest that perhaps a quark-diquark picture (with fewer degrees of freedom) could afford a more efficient description, although lattice simulation results provide no evidence for diquark clustering [15]. On the other hand, the missing states could simply have weak couplings to the  $\pi N$  system [1]. Such a case would present lattice QCD with a unique opportunity to complement experi-

mental searches for  $N^*$ 's, by identifying excited states not easily accessible to experiment (as in the case of glueballs or hybrids).

In attempting to answer these questions, one fact that will be clear is that it is not sufficient to look only at the standard low mass hadrons ( $\pi, \rho, N$  and  $\Delta$ ) on the lattice — one must consider the entire  $N^*$  (and in fact the entire excited baryon) spectrum. In this paper we present the first results of octet baryon mass simulations using an  $\mathcal{O}(a^2)$  improved gluon action and an improved Fat Link Irrelevant Clover (FLIC) [16] quark action in which only the irrelevant operators are constructed using fat links [17]. Configurations are generated on the Orion supercomputer at the University of Adelaide. After reviewing in Section II the main elements of lattice calculations of excited hadron masses and a brief overview of earlier calculations, we describe in Section III various features of interpolating fields used in this analysis. In Section IV we present results for  $J^P = \frac{1}{2}^\pm$  nucleons and hyperons. Finally, in Section V we make concluding remarks and discuss some future extensions of this work.

## II. EXCITED BARYONS ON THE LATTICE

The history of excited baryons on the lattice is quite brief, although recently there has been growing interest in finding new techniques to isolate excited baryons, motivated partly by the experimental  $N^*$  program at Jefferson Lab. The first comprehensive analysis of the positive parity excitation of the nucleon was performed by Leinweber [18] using Wilson fermions and an operator product expansion spectral ansatz. DeGrand and Hecht [19] used a “wave function technique” to access  $P$ -wave baryons. Later, Lee & Leinweber [20] introduced a parity projection technique to study the negative parity  $\frac{1}{2}^-$  states using an  $\mathcal{O}(a^2)$  tree-level tadpole-improved  $D_{\chi 34}$  quark action, and an  $\mathcal{O}(a^2)$  tree-level tadpole-improved gauge action. Following this, Lee [21] reported results using a  $D_{234}$  quark action with an improved gauge action on an anisotropic lattice to study the  $\frac{1}{2}^+$  and  $\frac{1}{2}^-$  excitations of the nucleon. The RIKEN-BNL group [22] has also performed an analysis of the  $N^*(\frac{1}{2}^-)$  and  $N'(\frac{1}{2}^+)$  excited states using domain wall fermions. More recently, a nonperturbatively improved clover quark action has been used by Richards et al. [23] to study the  $N^*(\frac{1}{2}^-)$  and  $\Delta^*(\frac{3}{2}^-)$  states.

Following standard notation, we define a two-point correlation function for a baryon  $B$  as

$$G_B(t, \vec{p}) \equiv \sum_{\vec{x}} e^{-i\vec{p}\cdot\vec{x}} \langle 0 | T \chi_B(x) \bar{\chi}_B(0) | 0 \rangle , \quad (1)$$

where  $\chi_B$  is a baryon interpolating field transforming positively under parity operation, and we have suppressed Dirac indices. The choice of interpolating field  $\chi_B$  is discussed in Section III below. The overlap of the field  $\chi_B$  with positive or negative parity states  $|B^\pm\rangle$  is parameterized by a coupling strength  $\lambda_{B^\pm}$

$$\langle 0 | \chi_B(0) | B^+(p, s) \rangle = \lambda_{B^+} \sqrt{\frac{M_{B^+}}{E_{B^+}}} u_{B^+}(p, s) , \quad (2a)$$

$$\langle 0 | \chi_B(0) | B^-(p, s) \rangle = \lambda_{B^-} \sqrt{\frac{M_{B^-}}{E_{B^-}}} \gamma_5 u_{B^-}(p, s) , \quad (2b)$$

where  $E_{B^\pm} = \sqrt{M_{B^\pm}^2 + \vec{p}^2}$  is the energy, and  $u_{B^\pm}(p, s)$  a Dirac spinor. For large Euclidean time, the correlation function can be written as a sum of the lowest energy positive and negative parity contributions

$$G_B(t, \vec{p}) \approx \lambda_{B^+}^2 \frac{(\gamma \cdot p + M_{B^+})}{2E_{B^+}} e^{-E_{B^+} t} + \lambda_{B^-}^2 \frac{(\gamma \cdot p - M_{B^-})}{2E_{B^-}} e^{-E_{B^-} t}, \quad (3)$$

when a fixed boundary condition in the time direction is used to remove backward propagating states. The positive and negative parity states are isolated by taking the trace of  $G_B$  with the operator  $\Gamma_\pm$ , where

$$\Gamma_\pm = \frac{1}{2} \left( 1 \pm \frac{M_{B^\pm}}{E_{B^\pm}} \gamma_4 \right). \quad (4)$$

For  $\vec{p} = 0$ ,  $E_{B^\pm} = M_{B^\pm}$  and using the operator  $\Gamma_\pm$  we can isolate the mass,  $M_{B^\pm}$ , of the baryon  $B^\pm$ . In this case, positive parity states propagate in the (1, 1) and (2, 2) elements of the Dirac matrix of Eq. (3), while negative parity states propagate in the (3, 3) and (4, 4) elements.

The baryon effective-mass function is defined by

$$M_B(t + 1/2) = \log[G_B(t, \vec{0})] - \log[G_B(t + 1, \vec{0})]. \quad (5)$$

At  $\vec{p} = 0$  we see that  $\Gamma_\pm^2 = \Gamma_\pm$  and  $\Gamma_\pm$  are then parity projectors. Meson masses are determined via analogous standard procedures. Five masses are used in the calculations [16] and the strange quark mass is taken to be the second heaviest quark mass in each case.

### III. INTERPOLATING FIELDS

In this analysis we consider two types of interpolating fields which have been used in the literature. The notation adopted follows that of Leinweber *et al.* [24]. For the positive parity proton we use as interpolating fields

$$\chi_1^{p+}(x) = \epsilon_{abc} \left( u_a^T(x) C \gamma_5 d_b(x) \right) u_c(x), \quad (6)$$

and

$$\chi_2^{p+}(x) = \epsilon_{abc} \left( u_a^T(x) C d_b(x) \right) \gamma_5 u_c(x), \quad (7)$$

where the fields  $u, d$  are evaluated at Euclidean space-time point  $x$ ,  $C$  is the charge conjugation matrix,  $a, b$  and  $c$  are color labels, and where the superscript  $T$  denotes the transpose. The neutron interpolating field is obtained via the exchange  $u \leftrightarrow d$ . As pointed out by Leinweber [18], because of the Dirac structure of the “diquark” in the parentheses in Eq.(6), the field  $\chi_1^{p+}$  involves both products of *upper*  $\times$  *upper*  $\times$  *upper* and *lower*  $\times$  *lower*  $\times$  *upper* components of spinors for positive parity baryons, so that in the nonrelativistic limit  $\chi_1^{p+} = \mathcal{O}(1)$ . We use the Dirac representation of the  $\gamma$  matrices here. Furthermore, since the “diquark” couples to a total spin 0, one expects an attractive force between the two quarks, and hence a lower energy state than for a state in which two quarks do not couple to spin 0.

The  $\chi_2^{p+}$  interpolating field, on the other hand, is known to have little overlap with the ground state [18,25]. Inspection of the structure of the Dirac matrices in Eq.(7) reveals that it involves only products of *upper*  $\times$  *lower*  $\times$  *lower* components for positive parity baryons, so that  $\chi_2^{p+} = \mathcal{O}(p^2/E^2)$  vanishes in the nonrelativistic limit. As a result of the mixing, the “diquark” term contains a factor  $\vec{\sigma} \cdot \vec{p}$ , meaning that the quarks no longer couple to spin 0, but are in a relative  $L = 1$  state. One expects therefore that two-point correlation functions constructed from the interpolating field  $\chi_2^{p+}$  are dominated by larger mass states than those arising from  $\chi_1^{p+}$  at early Euclidean times.

While the masses of negative parity baryons can be and are obtained directly from the (positive parity) interpolating fields in Eqs.(6) and (7) by using the parity projectors  $\Gamma_{\pm}$ , it is instructive nevertheless to examine the general properties of the negative parity interpolating fields. Interpolating fields for a negative parity proton can be constructed by multiplying the positive parity fields by  $\gamma_5$ ,  $\chi^{B-} \equiv \gamma_5 \chi^{B+}$ . In contrast to the positive parity case, both the interpolating fields  $\chi_1^{p-}$  and  $\chi_2^{p-}$  mix upper and lower components, and consequently both  $\chi_1^{p-}$  and  $\chi_2^{p-}$  are  $\mathcal{O}(p/E)$ .

Physically, two nearby  $J^P = \frac{1}{2}^-$  states are observed in the nucleon spectrum. In simple quark models, the splitting of these two orthogonal states is largely attributed to the extent to which scalar diquark configurations compose the wave function. It is reasonable to expect  $\chi_1^{p-}$  to have better overlap with scalar diquark dominated states, and thus provide a lower effective mass in the large Euclidean time regime explored in lattice simulations. If the effective mass associated with the  $\chi_2^{p-}$  correlator is larger, then this would be evidence of significant overlap of  $\chi_2^{p-}$  with the higher lying  $N^{\frac{1}{2}-}$  states. In this event, further analysis directed at resolving these two states is warranted.

Interpolating fields for the other members of the flavor SU(3) octet are constructed along similar lines. For the positive parity  $\Sigma^0$  hyperon one has [24]

$$\chi_1^{\Sigma}(x) = \frac{1}{\sqrt{2}} \epsilon_{abc} \left\{ \left( u_a^T(x) C \gamma_5 s_b(x) \right) d_c(x) + \left( d_a^T(x) C \gamma_5 s_b(x) \right) u_c(x) \right\} , \quad (8)$$

and similarly for the  $\chi_2^{\Sigma}$  field. Other charge states are obtained by  $d \rightarrow u$  or  $u \rightarrow d$ . Notice that  $\chi_1^{\Sigma}$  transforms as a triplet under SU(2) isospin. An SU(2) singlet interpolating field can be constructed by replacing “+”  $\rightarrow$  “−” in Eq.(8). For the SU(3) octet  $\Lambda$  interpolating field (denoted by “ $\Lambda^8$ ”), one has

$$\begin{aligned} \chi_1^{\Lambda^8}(x) = \frac{1}{\sqrt{6}} \epsilon_{abc} \left\{ 2 \left( u_a^T(x) C \gamma_5 d_b(x) \right) s_c(x) + \left( u_a^T(x) C \gamma_5 s_b(x) \right) d_c(x) \right. \\ \left. - \left( d_a^T(x) C \gamma_5 s_b(x) \right) u_c(x) \right\} , \end{aligned} \quad (9)$$

and similarly for  $\chi_2^{\Lambda^8}$  by simply moving the  $\gamma_5$  in each of the terms as was done to obtain Eq.(7) from Eq.(6).

The interpolating field for the SU(3) flavor singlet (denoted by “ $\Lambda^1$ ”) is given by [24]

$$\begin{aligned} \chi_1^{\Lambda^1}(x) = -2 \epsilon_{abc} \left\{ - \left( u_a^T(x) C \gamma_5 d_b(x) \right) s_c(x) + \left( u_a^T(x) C \gamma_5 s_b(x) \right) d_c(x) \right. \\ \left. - \left( d_a^T(x) C \gamma_5 s_b(x) \right) u_c(x) \right\} , \end{aligned} \quad (10)$$

where the last two terms are common to both  $\chi_1^{\Lambda^8}$  and  $\chi_1^{\Lambda^1}$ . In order to test the extent to which SU(3) flavor symmetry is valid in the baryon spectrum, one can construct another combined interpolating field composed of the terms common to  $\Lambda^1$  and  $\Lambda^8$ , which does not make any assumptions about SU(3) flavor symmetry properties of  $\Lambda$ . We define

$$\chi_1^{\Lambda^c}(x) = \frac{1}{\sqrt{2}} \epsilon_{abc} \left\{ \left( u_a^T(x) C \gamma_5 s_b(x) \right) d_c(x) - \left( d_a^T(x) C \gamma_5 s_b(x) \right) u_c(x) \right\} , \quad (11)$$

to be our “common” interpolating field which is the isosinglet analogue of  $\chi_1^\Sigma$  in Eq. (8). We similarly construct  $\chi_2^{\Lambda^1}$  and  $\chi_2^{\Lambda^c}$ . Such an interpolating field may be useful in determining the nature of the  $\Lambda^*(1405)$  resonance as it allows for mixing between singlet and octet states induced by SU(3) flavor symmetry breaking. Finally, the strangeness  $-2$ ,  $\Xi$  interpolating field is obtained by replacing the doubly represented  $u$  or  $d$  quark fields in Eqs. (6) and (7) by  $s$  quark fields.

#### IV. RESULTS

The calculations of octet excited baryon masses are performed on a  $16^3 \times 32$  lattice at  $\beta = 4.60$ , which corresponds to a lattice spacing of  $a = 0.125(2)$  fm set by the string tension with  $\sqrt{\sigma} = 440$  MeV. The analysis is based on a sample of 200 configurations. For the gauge fields, a mean-field improved plaquette plus rectangle action is used, while for the quark fields, a Fat-Link Irrelevant Clover (FLIC) [16] action is implemented. The use of fat links [17] in the irrelevant operators removes the need to fine tune the clover coefficient to remove  $\mathcal{O}(a)$  artifacts. In the present simulations we employ a highly improved definition of  $F_{\mu\nu}$  [16,26] leaving errors of  $\mathcal{O}(a^6)$ . Mean-field improvement of the tree-level clover coefficient with fat links represents a small correction and proves to be adequate [16]. The fattening, or smearing of the lattice links with their nearest neighbors, reduces the problem of exceptional configurations, and minimizes the effect of renormalization on the action improvement terms. By smearing only the irrelevant, higher dimensional terms in the action, and leaving the relevant dimension-four operators untouched, we retain short distance quark and gluon interactions at the scale of the cutoff. Although the simulations are performed both with  $n = 4$  and 12 smearing sweeps at  $\alpha = 0.7$ , the improved gauge fields are found to be somewhat smooth after only 4 sweeps. Since the results with  $n = 4$  sweeps exhibit slightly better scaling than those with  $n = 12$  [16], we focus on the results with 4 smearing sweeps. The 12-sweep results are consistent with all our conclusions. Further details of the simulations are given in Ref. [16].

A fixed boundary condition in the time direction is used for the fermions by setting  $U_t(\vec{x}, N_t) = 0 \ \forall \ \vec{x}$  in the hopping terms of the fermion action, with periodic boundary conditions imposed in the spatial directions. Gauge-invariant gaussian smearing [27] in the spatial dimensions is applied at the source to increase the overlap of the interpolating operators with the ground states.

Figure 1 shows the positive and negative parity nucleon effective mass plots for both  $\chi_1$  and  $\chi_2$  interpolating fields for the FLIC action. The effective mass plots for the other hadrons are similar, and all display acceptable plateau behavior. Good values of covariance matrix based  $\chi^2/N_{\text{DF}}$  are obtained for the ground state nucleon ( $N_1$ ) for many different

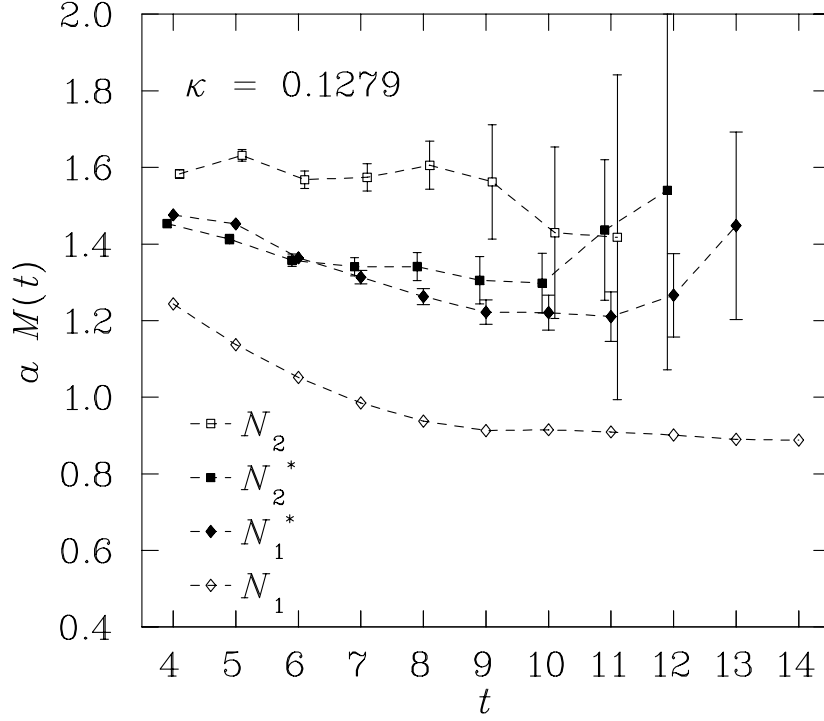


FIG. 1. Effective masses of the lowest lying positive and negative parity nucleon states using the FLIC action defined with 4 sweeps of smearing at  $\alpha = 0.7$ . The  $J^P = \frac{1}{2}^+$  ( $\frac{1}{2}^-$ ) states labeled  $N_1$  ( $N_1^*$ ) and  $N_2$  ( $N_2^*$ ) are obtained using the  $\chi_1$  and  $\chi_2$  interpolating fields, respectively.

time-fitting intervals as long as one fits after time slice 8. All fits for the positive parity states obtained with the  $\chi_1$  interpolating fields for this action are therefore performed on time slices 9 through 14. The lowest  $J^P = \frac{1}{2}^-$  excitation for the  $\chi_1$  interpolating field ( $N_1^*$ ) uses time slices 9–12. The states obtained from the  $\chi_2$  interpolating field, however, plateau at earlier times and are also subject to noise earlier in time than the states obtained with the  $\chi_1$  field. For these reasons, good values of  $\chi^2/N_{\text{DF}}$  are obtained on the time interval 6–8 for both positive and negative parity states.

In Fig. 2 we show the nucleon and  $N^*(\frac{1}{2}^-)$  masses as a function of the pseudoscalar meson mass squared,  $m_\pi^2$ . The results of the new simulations, using the  $\chi_1$  interpolating field, Eq. (6), are indicated by the filled squares for the FLIC action, and by the stars for the Wilson action (the Wilson points are obtained from a sample of 50 configurations). The values of  $m_\pi^2$  correspond to  $\kappa$  values given in Table I.

For comparison, we also show results from earlier simulations with domain wall fermions (DWF) [22] (open triangles), and a nonperturbatively (NP) improved clover action at  $\beta = 6.2$  [23]. The scatter of the different NP improved results is due to different source smearing and volume effects: the open squares are obtained by using fuzzed sources and local sinks, the open circles use Jacobi smearing at both the source and sink, while the open diamonds, which extend to smaller quark masses, are obtained from a larger lattice ( $32^3 \times 64$ ) using Jacobi smearing. The empirical masses of the nucleon and the three lowest  $\frac{1}{2}^-$  excitations

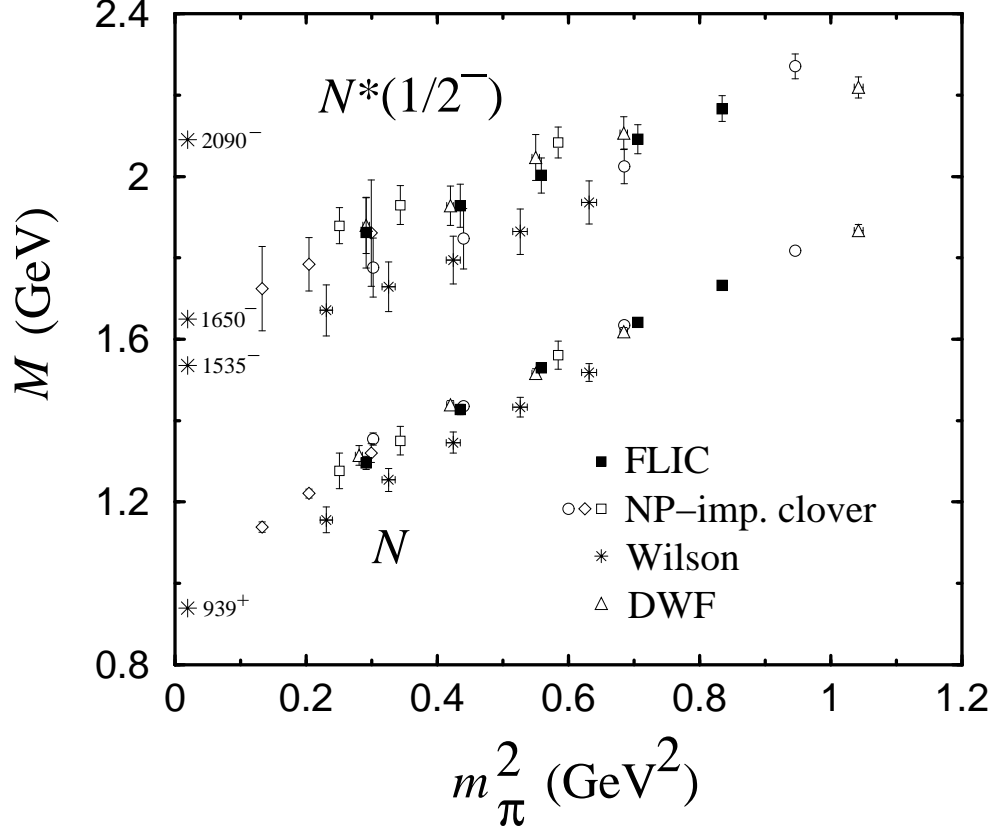


FIG. 2. Masses of the nucleon ( $N$ ) and the lowest  $J^P = \frac{1}{2}^-$  excitation (“ $N^*$ ”), obtained from the  $\chi_1$  interpolating field. The FLIC and Wilson results are from the present analysis, with the DWF [22] and NP improved clover [23] results shown for comparison. The empirical nucleon and low lying  $N^*(\frac{1}{2}^-)$  masses are indicated by the asterisks along the ordinate.

$\kappa$	$m_\pi a$	$m_{N_1} a$	$m_{N_1^*} a$	$m_{N_2^*} a$	$m_{N_2} a$
0.1260	0.5797(23)	1.0995(58)	1.375(20)	1.453(11)	1.674(17)
0.1266	0.5331(24)	1.0419(64)	1.327(23)	1.416(12)	1.638(19)
0.1273	0.4744(27)	0.9709(72)	1.271(27)	1.376(15)	1.600(22)
0.1279	0.4185(30)	0.9055(82)	1.224(34)	1.351(19)	1.573(26)
0.1286	0.3429(37)	0.8220(102)	1.182(55)	1.347(29)	1.560(37)

TABLE I. Values of  $\kappa$  used in this analysis and the corresponding  $\pi$ ,  $N_1$ ,  $N_1^*$ ,  $N_2^*$  and  $N_2$  masses for the FLIC action with 4 sweeps of smearing at  $\alpha = 0.7$ . Here  $\kappa_{\text{cr}} = 0.1300$ , and a string tension analysis provides  $a = 0.125(2)$  fm for  $\sqrt{\sigma} = 440$  MeV.



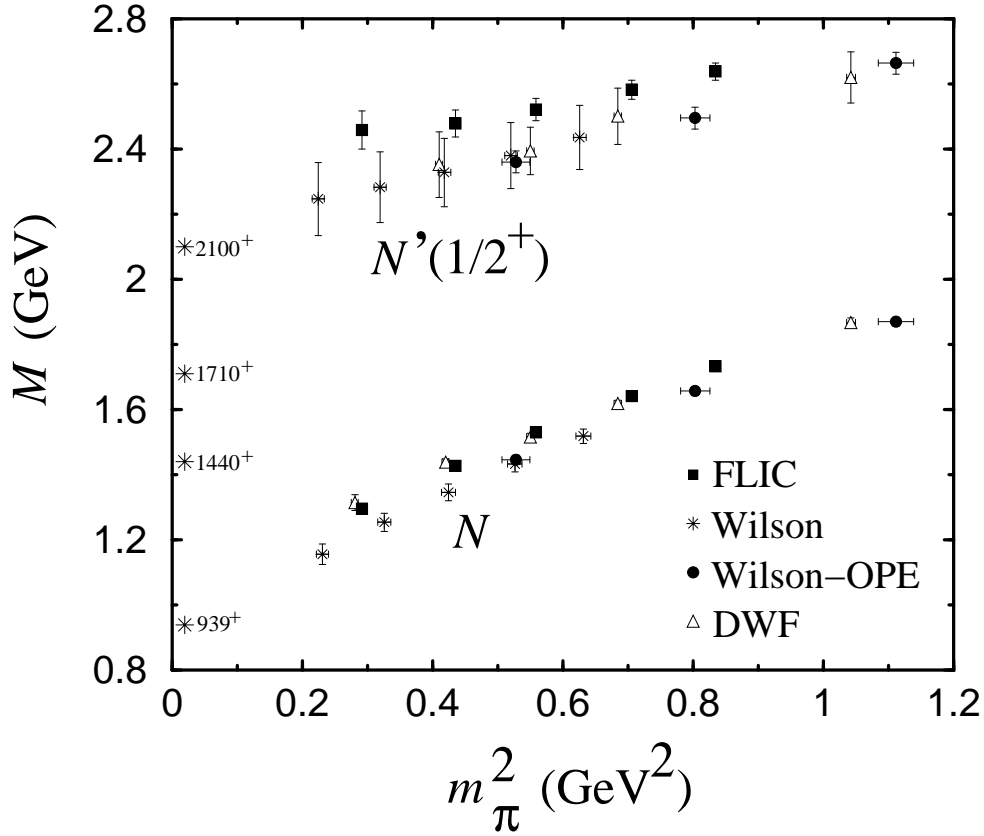


FIG. 3. Masses of the nucleon, and the lowest  $J^P = \frac{1}{2}^+$  excitation (“ $N'$ ”) obtained from the  $\chi_2$  interpolating field. The FLIC results are compared with the earlier DWF [22] and Wilson-OPE [18] analyses, as well as with the Wilson results from this analysis. The empirical nucleon and low lying  $N^*(\frac{1}{2}^+)$  masses are indicated by asterisks.

are indicated by the asterisks along the ordinate.

There is excellent agreement between the different improved actions for the nucleon mass, in particular between the FLIC, DWF [22] and NP improved clover [23] results. On the other hand, the Wilson results lie systematically low in comparison to these due to the large  $\mathcal{O}(a)$  errors in this action [16]. A similar pattern is repeated for the  $N^*(\frac{1}{2}^-)$  masses. Namely, the FLIC, DWF and NP improved clover masses are in good agreement with each other, while the Wilson results again lie systematically lower. A mass splitting of around 400 MeV is clearly visible between the  $N$  and  $N^*$  for all actions, including the Wilson action, despite its poor chiral properties. Furthermore, the trend of the  $N^*(\frac{1}{2}^-)$  data with decreasing  $m_\pi$  is consistent with the mass of the lowest lying physical negative parity  $N^*$  states.

Figure 3 shows the mass of the first  $J^P = \frac{1}{2}^+$  excitation of the nucleon (denoted by “ $N'(1/2^+)$ ”), constructed from the  $\chi_2$  interpolating field in Eq. (7). Data for the nucleon sector are provided in Table I. As is long known, the positive parity  $\chi_2$  interpolating field does not have good overlap with the nucleon ground state [18]. It has been speculated that

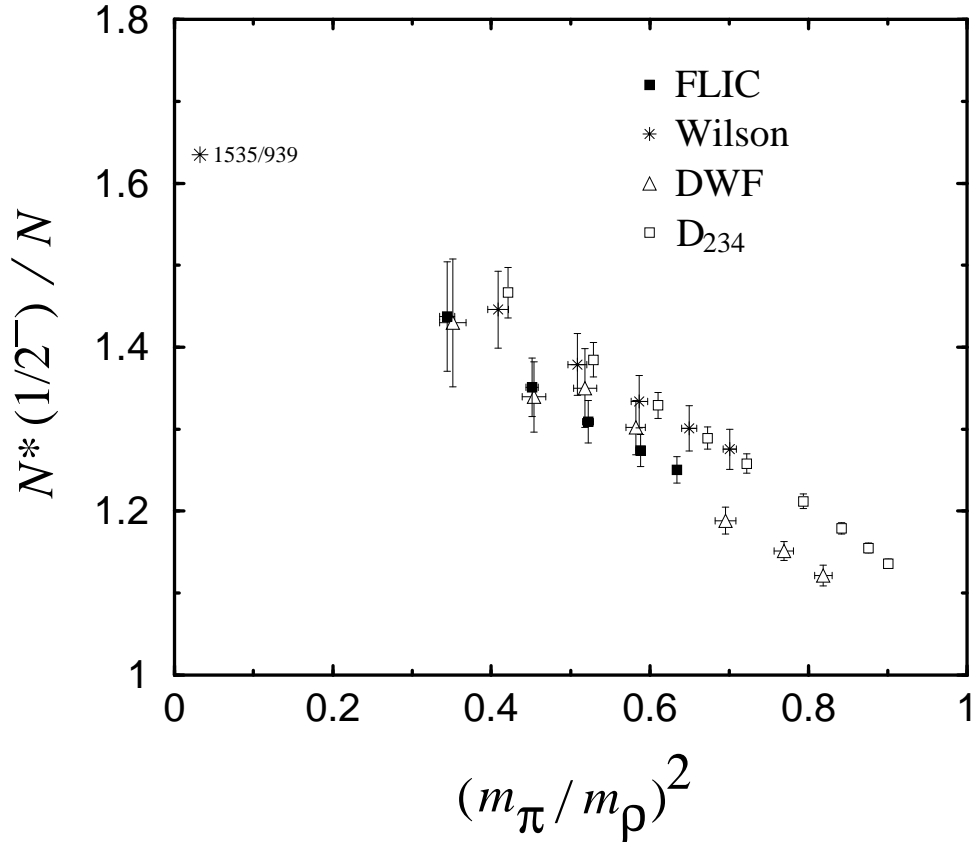


FIG. 4. Ratio of the ground state  $N^*(\frac{1}{2}^-)$  and nucleon masses, from the  $\chi_1$  interpolating field. The FLIC and Wilson results are from the present analysis, with results from the D234 [21] and DWF [22] actions shown for comparison. The empirical  $N^*(1535)/N$  mass ratio is denoted by the asterisk.

it may have overlap with the lowest  $\frac{1}{2}^+$  excited state, the  $N^*(1440)$  Roper resonance [22]. In addition to the FLIC and Wilson results from the present analysis, we also show in Fig. 3 the DWF results [22], and results from an earlier analysis with Wilson fermions together with the operator product expansion [18]. The physical values of the lowest three  $\frac{1}{2}^+$  excitations of the nucleon are indicated by the asterisks.

The most striking feature of the data is the relatively large excitation energy of the  $N'$ , some 1 GeV above the nucleon. There is little evidence, therefore, that this state is the  $N^*(1440)$  Roper resonance. While it is possible that the Roper resonance may have a strong nonlinear dependence on the quark mass at  $m_\pi^2 \lesssim 0.2 \text{ GeV}^2$ , arising from, for example, pion loop corrections, it is unlikely that this behavior would be so dramatically different from that of the  $N^*(1535)$  so as to reverse the level ordering obtained from the lattice. A more likely explanation is that the  $\chi_2$  interpolating field does not have good overlap with either the nucleon or the  $N^*(1440)$ , but rather a (combination of) excited  $\frac{1}{2}^+$  state(s).

Recall that in a constituent quark model in a harmonic oscillator basis, the mass of

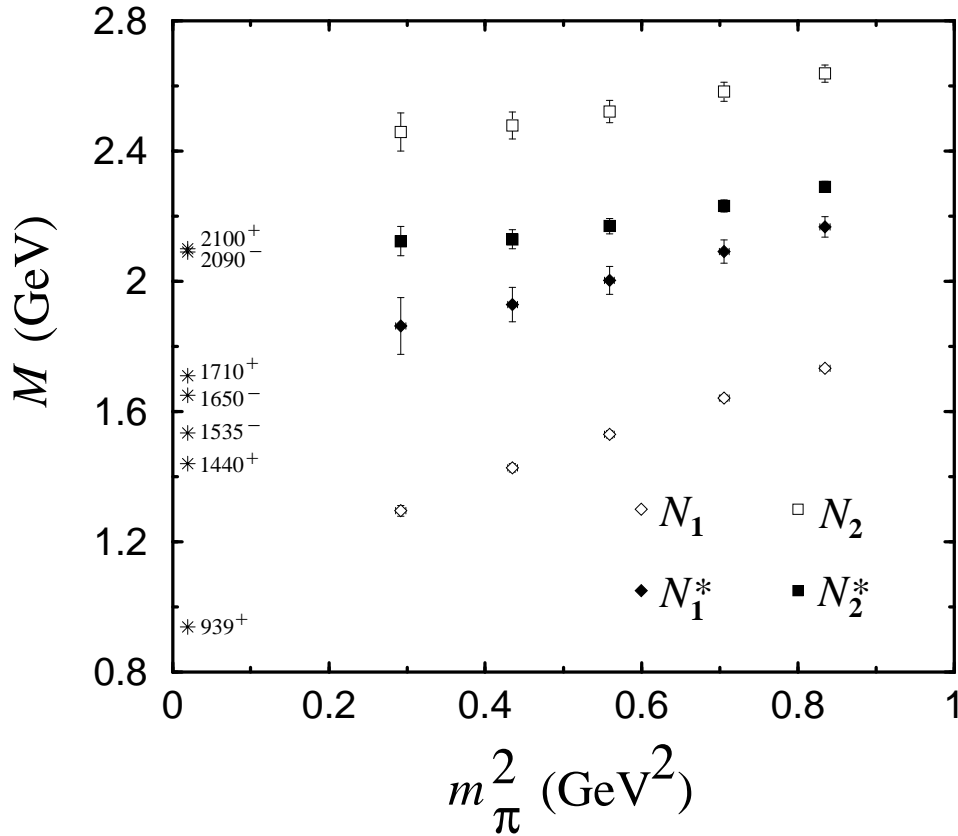


FIG. 5. Masses of the  $J^P = \frac{1}{2}^+$  and  $\frac{1}{2}^-$  nucleon states, for the FLIC action. The positive (negative) parity states labeled  $N_1$  ( $N_1^*$ ) and  $N_2$  ( $N_2^*$ ) are constructed from the  $\chi_1$  and  $\chi_2$  interpolating fields, respectively. Empirical masses of the low lying  $\frac{1}{2}^\pm$  states are indicated by the asterisks.

the lowest mass state with the Roper quantum numbers is higher than the lowest  $P$ -wave excitation. It seems that neither the lattice data (at large quark masses and with our interpolating fields) nor the constituent quark model have good overlap with the Roper resonance. Better overlap with the Roper is likely to require more exotic interpolating fields.

In Fig. 4 we show the ratio of the masses of the  $N^*(\frac{1}{2}^-)$  and the nucleon, using the  $\chi_1$  interpolating field. Once again, there is good agreement between the FLIC and DWF actions. However, the results for the Wilson action lie above the others, as do those for the anisotropic  $D_{234}$  action [21]. The  $D_{234}$  action has been mean-field improved, and uses an anisotropic lattice which is relatively coarse in the spatial direction ( $a \approx 0.24$  fm). This is perhaps an indication of the need for nonperturbative or fat-link improvement.

The mass splitting between the two lightest  $N^*(\frac{1}{2}^-)$  states ( $N^*(1535)$  and  $N^*(1650)$ ) can be studied by considering the odd parity content of the  $\chi_1$  and  $\chi_2$  interpolating fields in Eqs. (6) and (7). Recall that the “diquarks” in  $\chi_1$  and  $\chi_2$  couple differently to spin, so that even though the correlation functions built up from the  $\chi_1$  and  $\chi_2$  fields will be made up of a mixture of many excited states, they will have dominant overlap with different states,

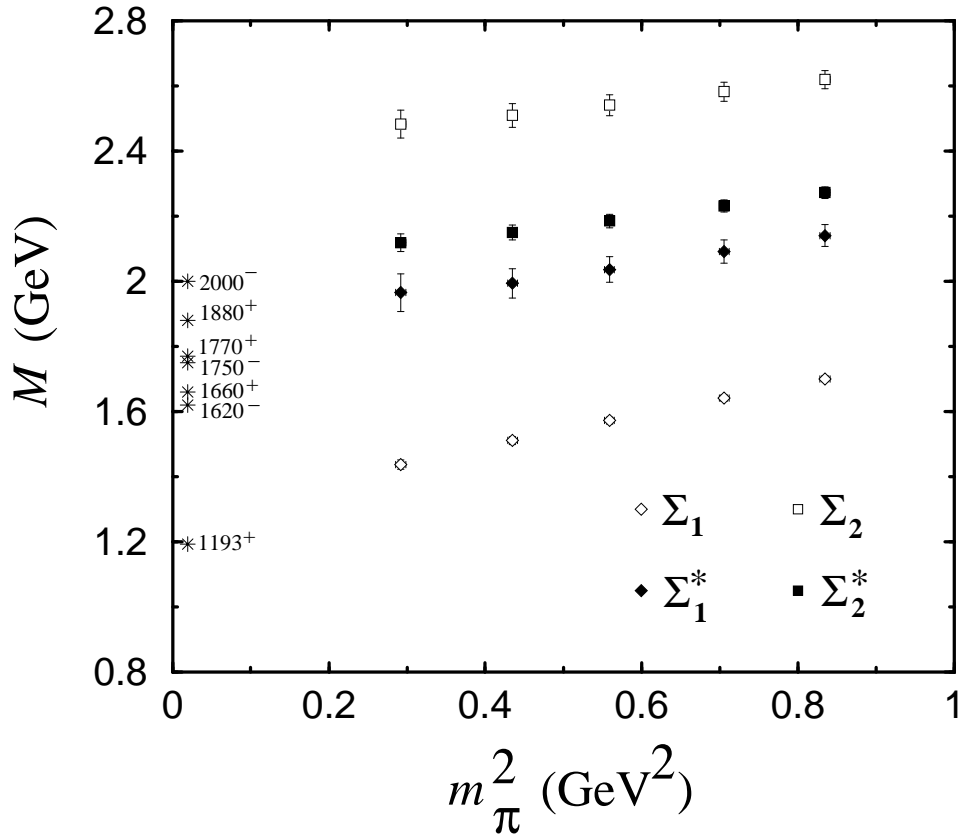


FIG. 6. As in Fig. 5 but for the  $\Sigma$  baryons.

yielding different masses [18,20]. The results, shown in Fig. 5 for the FLIC action, indicate that indeed the  $N^*(\frac{1}{2}^-)$  corresponding to the  $\chi_2$  field (labeled “ $N_2^*$ ”) lies above the  $N^*(\frac{1}{2}^-)$  associated with the  $\chi_1$  field (“ $N_1^*$ ”). The masses of the corresponding positive parity states, associated with the  $\chi_1$  and  $\chi_2$  fields (labeled “ $N_1$ ” and “ $N_2$ ”, respectively) are shown for comparison. For reference, we also list the empirical values of the low lying  $\frac{1}{2}^\pm$  states. It is interesting to note that the mass splitting between the positive parity  $N_1$  and negative parity  $N_{1,2}^*$  states (roughly 400–500 MeV) is similar to that between the  $N_{1,2}^*$  and the positive parity  $N_2$  state, reminiscent of a constituent quark–harmonic oscillator picture.

Turning to the strange sector, in Fig. 6 we show the masses of the positive and negative parity  $\Sigma$  baryons calculated from the FLIC action, and compared with the physical masses of the known positive and negative parity states. The data for these states are listed in Table II. The pattern of mass splittings is similar to that found in Fig. 5 for the nucleon. Namely, the  $\frac{1}{2}^+$  state associated with the  $\chi_1$  field appears consistent with the empirical  $\Sigma(1193)$  ground state, while the  $\frac{1}{2}^+$  state associated with the  $\chi_2$  field lies significantly above the observed first (Roper-like)  $\frac{1}{2}^+$  excitation,  $\Sigma^*(1660)$ . There is also evidence for a mass splitting between the negative parity states associated with the  $\chi_1$  and  $\chi_2$  operators, similar to that in the nonstrange sector.

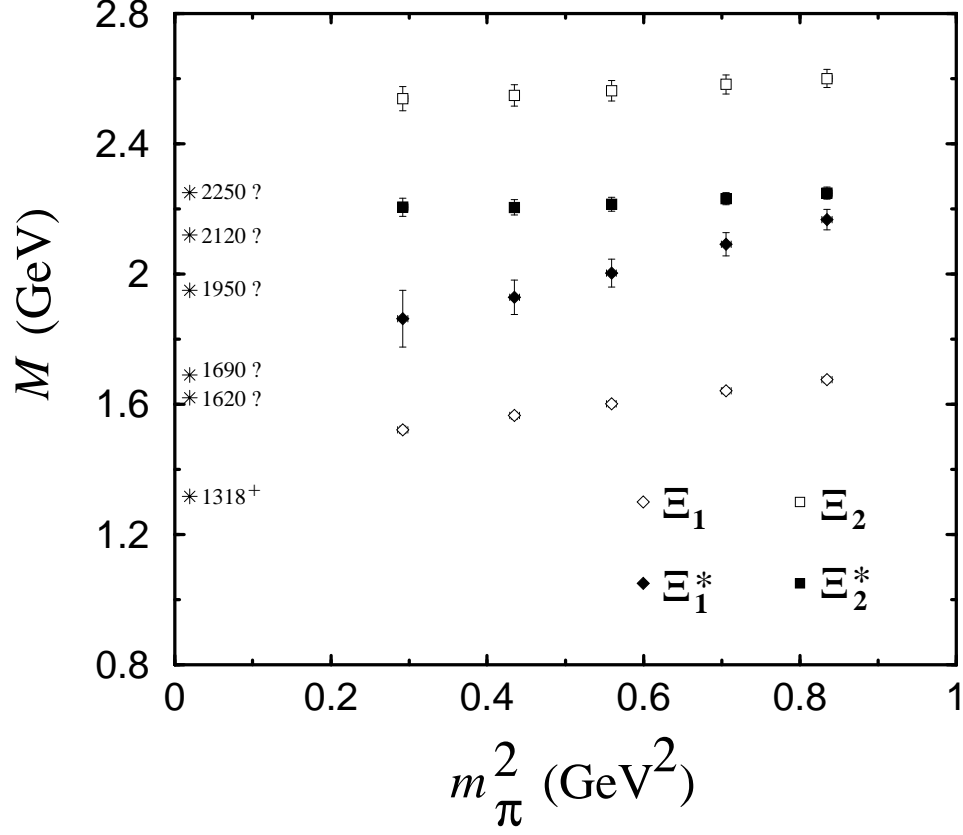


FIG. 7. As in Fig. 5 but for the  $\Xi$  baryons. The  $J^P$  values of the excited states marked with “?” are undetermined.

$\kappa$	$m_{\Sigma_1} a$	$m_{\Sigma_1^*} a$	$m_{\Sigma_2^*} a$	$m_{\Sigma_2} a$
0.1260	1.0789(60)	1.358(21)	1.442(11)	1.662(18)
0.1266	1.0419(64)	1.327(23)	1.416(12)	1.638(19)
0.1273	0.9977(69)	1.292(25)	1.387(13)	1.612(21)
0.1279	0.9587(76)	1.265(29)	1.364(15)	1.592(23)
0.1286	0.9120(89)	1.247(37)	1.344(17)	1.575(27)

TABLE II. As for Table I, but for the  $\Sigma$  states.

$\kappa$	$m_{\Xi_1} a$	$m_{\Xi_1^*} a$	$m_{\Xi_2^*} a$	$m_{\Xi_2} a$
0.1260	1.0631(62)	1.375(20)	1.427(11)	1.650(18)
0.1266	1.0419(64)	1.327(23)	1.416(12)	1.638(19)
0.1273	1.0162(66)	1.271(27)	1.405(13)	1.626(20)
0.1279	0.9933(69)	1.224(34)	1.399(15)	1.617(21)
0.1286	0.9654(74)	1.182(55)	1.399(18)	1.611(23)

TABLE III. As for Table I, but for the  $\Xi$  states.

$\kappa$	$m_{\Lambda_1} a$	$m_{\Lambda_1^*} a$	$m_{\Lambda_2^*} a$	$m_{\Lambda_2} a$
0.1260	1.0822(60)	1.360(21)	1.439(11)	1.662(17)
0.1266	1.0419(64)	1.327(23)	1.416(12)	1.638(19)
0.1273	0.9923(69)	1.288(26)	1.392(14)	1.613(21)
0.1279	0.9468(75)	1.253(30)	1.379(17)	1.596(24)
0.1286	0.8887(87)	1.214(38)	1.383(25)	1.589(30)

TABLE IV. As for Table I, but for the octet  $\Lambda^8$  states.

The spectrum of the strangeness  $-2$  positive and negative parity  $\Xi$  hyperons is displayed in Fig. 7, with data given in Table III. Once again, the pattern of calculated masses repeats that found for the  $\Sigma$  and  $N$  masses in Figs. 5 and 6. The empirical masses of the physical  $\Xi^*$  baryons are denoted by asterisks, however, for all but the ground state  $\Xi(1318)$ , the  $J^P$  values are not known.

Finally, in Fig. 8 we show the spectrum of positive and negative parity  $\Lambda$  hyperons for the FLIC action, with the data given in Tables IV and V. The positive (negative) parity states labeled  $\Lambda_1$  ( $\Lambda_1^*$ ) and  $\Lambda_2$  ( $\Lambda_2^*$ ) are constructed from the  $\chi_1^\Lambda$  and  $\chi_2^\Lambda$  interpolating fields, respectively. The  $\Lambda^8$  (octet) states are represented by the open symbols, while the isosinglet  $\Lambda^c$  states (made up of terms common to both the octet and singlet fields) are denoted by the filled symbols. The empirical  $\Lambda^*(\frac{1}{2}^\pm)$  masses are denoted by asterisks.

A similar pattern of mass splittings is observed to that for the  $N^*$ 's in Fig. 5. In particular, the negative parity  $\Lambda_1^*$  state (squares) lies  $\sim 400$  MeV above the positive parity  $\Lambda_1$  ground state (diamonds), for both the  $\Lambda^8$  and  $\Lambda^c$  fields. There is also clear evidence of a mass splitting between the  $\Lambda_1^*$  (squares) and  $\Lambda_2^*$  (triangles), especially for the  $\Lambda^8$  field (open symbols), which may indicate sensitivity to the physics responsible for the mass splitting between the negative parity  $\Lambda^*(1670)$  and  $\Lambda^*(1800)$  states. The fact that the  $\Lambda_2^*$  appears at a higher energy than the  $\Lambda_1^*$  can be attributed to the fact that the latter contains a “diquark” combination coupled to spin 0 (c.f. the masses of the  $N_1^*(\frac{1}{2}^-)$  and  $N_2^*(\frac{1}{2}^-)$  in Fig. 5).

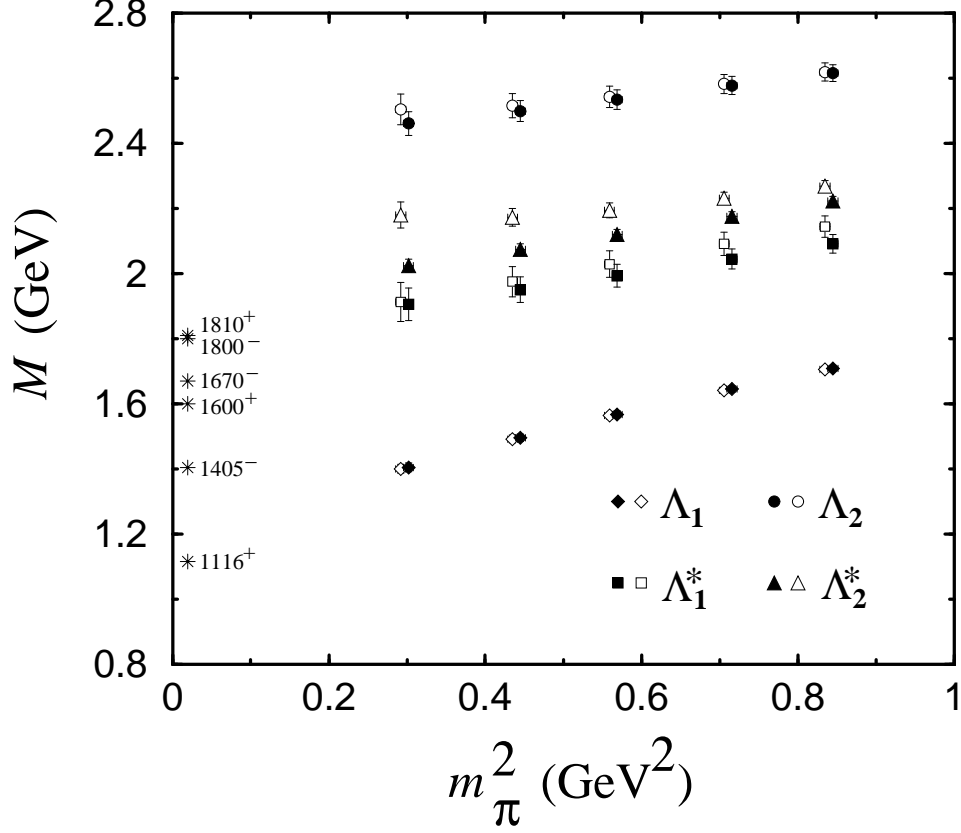


FIG. 8. Masses of the positive and negative parity  $\Lambda$  states, for the octet  $\Lambda^8$  (open symbols) and “common”  $\Lambda^c$  (filled symbols) interpolating fields with the FLIC action. The positive (negative) parity states labeled  $\Lambda_1$  ( $\Lambda_1^*$ ) and  $\Lambda_2$  ( $\Lambda_2^*$ ) are constructed from the  $\chi_1^\Lambda$  and  $\chi_2^\Lambda$  interpolating fields, respectively. Empirical masses of the low lying  $\frac{1}{2}^\pm$  states are indicated by the asterisks.

$\kappa$	$m_{\Lambda_1}a$	$m_{\Lambda_1^*}a$	$m_{\Lambda_2^*}a$	$m_{\Lambda_2}a$
0.1260	1.0845(59)	1.327(18)	1.410(9)	1.660(17)
0.1266	1.0442(63)	1.298(20)	1.380(9)	1.635(17)
0.1273	0.9947(68)	1.265(22)	1.345(10)	1.608(19)
0.1279	0.9493(75)	1.238(25)	1.316(11)	1.586(20)
0.1286	0.8914(86)	1.209(32)	1.284(12)	1.561(23)

TABLE V. As for Table I, but for the “common”  $\Lambda^c$  states.

On the other hand, the analogous splitting for the  $\Lambda^c$  field is considerably smaller, which is consistent with the existence of only one low mass SU(3)-flavor singlet  $\frac{1}{2}^-$  state ( $\Lambda^*(1405)$ ) but two octet  $\frac{1}{2}^-$  states ( $\Lambda^*(1670)$  and  $\Lambda^*(1800)$ ). As for the other baryons, there is little evidence that the  $\Lambda_2$  (circles) has any significant overlap with the first positive parity excited state,  $\Lambda^*(1600)$  (c.f. the Roper resonance,  $N^*(1440)$ , in Fig. 5).

While it seems plausible that nonanalyticities in a chiral extrapolation [7] of  $N_1$  and  $N_1^*$  results could eventually lead to agreement with experiment, the situation for the  $\Lambda^*(1405)$  is not as compelling. Whereas a 150 MeV pion-induced self energy is required for the  $N_1$ ,  $N_1^*$  and  $\Lambda_1$ , 400 MeV is required to approach the empirical mass of the  $\Lambda^*(1405)$ . This may not be surprising for the octet fields, as the  $\Lambda^*(1405)$ , being an SU(3) flavor singlet, may not couple strongly to an SU(3) octet interpolating field. This large discrepancy suggests that relevant physics may be absent from simulations in the quenched approximation. The behavior of the  $\Lambda_{1,2}^*$  states may be modified at small values of the quark mass through nonlinear effects associated with Goldstone boson loops including the strong coupling of the  $\Lambda^*(1405)$  to  $\Sigma\pi$  and  $\bar{K}N$  channels. While some of this coupling will survive in the quenched approximation, generally the couplings are modified and suppressed [8,28]. It is also interesting to note that the octet  $\Lambda_1^*$  and  $\Lambda_2^*$  masses display a similar behavior to that seen for the  $\Xi_1^*$  and  $\Xi_2^*$  states, which are dominated by the heavier strange quark. Alternatively, the study of more exotic interpolating fields may indicate the the  $\Lambda^*(1405)$  does not couple strongly to  $\chi_1$  or  $\chi_2$ . Investigations at lighter quark masses involving quenched chiral perturbation theory will assist in resolving these issues.

## V. CONCLUSION

We have presented the first results for the excited baryon spectrum from lattice QCD using an  $\mathcal{O}(a^2)$  improved gauge action and an improved Fat-Link Irrelevant Clover (FLIC) quark action in which only the links of the irrelevant dimension five operators are smeared. The simulations have been performed on a  $16^3 \times 32$  lattice at  $\beta = 4.60$ , providing a lattice spacing of  $a = 0.125(2)$  fm. The analysis is based on a set of 200 configurations generated on the Orion supercomputer.

Good agreement is obtained between the FLIC and other improved actions, such as the nonperturbatively improved clover [23] and domain wall fermion (DWF) [22] actions, for the nucleon and its chiral partner, with a mass splitting of  $\sim 400$  MeV. Our results for the  $N^*(\frac{1}{2}^-)$  improve on those using the  $D_{234}$  [21] and Wilson actions. Despite strong chiral symmetry breaking, the results with the Wilson action are still able to resolve the splitting between the chiral partners of the nucleon. Using the two standard nucleon interpolating fields, we also confirm earlier observations [20] of a mass splitting between the two nearby  $\frac{1}{2}^-$  states. We find no evidence of overlap with the  $\frac{1}{2}^+$  Roper resonance.

In the strange sector, we have investigated the overlap of various  $\Lambda$  interpolating fields with the low lying  $\frac{1}{2}^\pm$  states. Once again a clear mass splitting of  $\sim 400$  MeV between the octet  $\Lambda$  and its parity partner is seen, with some evidence of a mass splitting between the two states primarily associated with the octet  $\Lambda_1^*$  and  $\Lambda_2^*$  interpolating fields. The latter splitting is significantly reduced for the  $\Lambda^c$  correlator, which does not make any assumptions about the SU(3) flavor symmetry properties of the  $\Lambda$ . We find no evidence of strong overlap



with the  $\frac{1}{2}^+$  “Roper” excitation,  $\Lambda^*(1600)$ . The empirical mass suppression of the  $\Lambda^*(1405)$  is not evident in these quenched QCD simulations, possibly suggesting an important role for the meson cloud of the  $\Lambda^*(1405)$  and/or a need for more exotic interpolating fields.

We have not attempted to extrapolate the lattice results to the physical region of light quarks, since the nonanalytic behavior of  $N^*$ ’s near the chiral limit is not as well studied as that of the nucleon [7,8]. It is vital that future lattice  $N^*$  simulations push closer towards the chiral limit. On a promising note, our simulations with the 4 sweep FLIC action are able to reach relatively low quark masses ( $m_q \sim 60\text{--}70$  MeV) already. Our discussion of quenching effects is limited to a qualitative level until the formulation of quenched chiral perturbation theory for  $\frac{1}{2}^-$  baryon resonances is established [29] or dynamical fermion simulations are completed. Experience suggests that dynamical fermion results will be shifted down in mass relative to quenched results, with increased downward curvature near the chiral limit [8]. It will be fascinating to confront this physics with both numerical simulation and chiral nonanalytic approaches.

Having firmly established the different behavior of  $N_1^*$  and  $N_2^*$  effective masses we intend to use variational techniques to better resolve individual excited states. In particular, we plan to consider  $N_1^*$  and  $N_2^*$  fields (using a  $2 \times 2$  correlation matrix), and the  $\Lambda^8$ ,  $\Lambda^c$  and  $\Lambda^1$  states (with a  $3 \times 3$  matrix). In order to further explore the origin of the Roper resonances or the  $\Lambda^*(1405)$ , more exotic interpolating fields involving higher Fock states, or nonlocal operators should be investigated. Finally, the present  $N^*$  mass analysis will be extended in future to include  $N \rightarrow N^*$  transition form factors through the calculation of three-point correlation functions.

## ACKNOWLEDGMENTS

We thank Waseem Kamleh, Tony Thomas and Ross Young for beneficial discussions. Thanks to D.G. Richards for interesting discussions and for providing the data points from Ref. [23]. This work was supported by the Australian Research Council, and the U.S. Department of Energy contract DE-AC05-84ER40150, under which the Southeastern Universities Research Association (SURA) operates the Thomas Jefferson National Accelerator Facility (Jefferson Lab). The calculations reported here were carried out on the Orion supercomputer at the Australian National Computing Facility for Lattice Gauge Theory (NCFLGT) at the University of Adelaide.

## REFERENCES

- [1] S. Capstick and W. Roberts, nucl-th/0008028.
- [2] N. Isgur and G. Karl, Phys. Lett. B **72** (1977) 109; Phys. Rev. D **19** (1979) 2653; N. Isgur, *ibid* **62** (2000) 054026; nucl-th/0007008.
- [3] P.A.M. Guichon, Phys. Lett. B **164** (1985) 361.
- [4] O. Krehl, C. Hanhart, S. Krewald and J. Speth, Phys. Rev. C **62** (2000) 025207.
- [5] Z.-P. Li, V. Burkert and Z.-J. Li, Phys. Rev. D **46** (1992) 70; C.E. Carlson and N.C. Mukhopadhyay, Phys. Rev. Lett. **67** (1991) 3745.
- [6] R.H. Dalitz and J.G. McGinley, in *Low and Intermediate Energy Kaon-Nucleon Physics*, ed. E. Ferarri and G. Violini (Reidel, Boston, 1980), p.381; R.H. Dalitz, T.C. Wong and G. Rajasekaran, Phys. Rev. **153** (1967) 1617; E.A. Veit, B.K. Jennings, R.C. Barrett and A.W. Thomas, Phys. Lett. B **137** (1984) 415; E.A. Veit, B.K. Jennings, A.W. Thomas and R.C. Barrett, Phys. Rev. D **31** (1985) 1033; P.B. Siegel and W. Weise, Phys. Rev. C **38** (1988) 2221; N. Kaiser, P.B. Siegel and W. Weise, Nucl. Phys. **A594** (1995) 325; E. Oset, A. Ramos and C. Bennhold, nucl-th/0109006.
- [7] D.B. Leinweber, A.W. Thomas, K. Tsushima and S.V. Wright, Phys. Rev. D **61** (2000) 074502.
- [8] R. D. Young, D. B. Leinweber, A. W. Thomas and S. V. Wright, hep-lat/0111041.
- [9] L.Y. Glozman and D.O. Riska, Phys. Rep. **268** (1996) 263.
- [10] N. Isgur, Phys. Rev. D **62** (2000) 054026.
- [11] A.W. Thomas and G. Krein, Phys. Lett. B **456** (1999) 5; *ibid.* **B** 481 (2000) 21.
- [12] S. Capstick and N. Isgur, Phys. Rev. D **34** (1986) 2809.
- [13] C.L. Schat, J.L. Goity and N.N. Scoccola, hep-ph/0111082; C.E. Carlson, C.D. Carone, J.L. Goity and R.F. Lebed, Phys. Rev. D **59** (1999) 114008; J.L. Goity, Phys. Lett. B **414** (1997) 140.
- [14] D.B. Leinweber, Ann. Phys. **198** (1990) 203.
- [15] D.B. Leinweber, Phys. Rev. D **47** (1993) 5096.
- [16] J.M. Zanotti *et al.*, to appear in Phys. Rev. D, hep-lat/0110216; Proceedings of the Workshop on Lattice Hadron Physics, Cairns, Australia (July, 2001), hep-lat/0201004.
- [17] T. DeGrand, Phys. Rev. D **60** (1999) 094501.
- [18] D.B. Leinweber, Phys. Rev. D **51** (1995) 6383.
- [19] T. A. DeGrand and M. W. Hecht, Phys. Rev. D **46**, 3937 (1992) [arXiv:hep-lat/9206011].
- [20] F.X. Lee and D.B. Leinweber, Nucl. Phys. Proc. Suppl. **73** (1999) 258.
- [21] F.X. Lee, Nucl. Phys. Proc. Suppl. **94** (2001) 251.
- [22] S. Sasaki, T. Blum and S. Ohta, hep-lat/0102010; S. Sasaki, hep-lat/0110052.
- [23] D.G. Richards, Nucl. Phys. Proc. Suppl. **94** (2001) 269; M. Göckeler *et al.*, hep-lat/0106022; D.G. Richards *et al.*, hep-lat/0112031.
- [24] D.B. Leinweber, R.W. Woloshyn and T. Draper, Phys. Rev. D **43** (1991) 1659.
- [25] K. Bowler *et al.*, Nucl. Phys. **B240** (1984) 213.
- [26] S. Bilson-Thompson *et al.*, in Proceedings of the Workshop on Lattice Hadron Physics, Cairns, Australia (July, 2001), hep-lat/0112034; and in preparation.
- [27] S. Gusken, Nucl. Phys. Proc. Suppl. **17** (1990) 361.
- [28] J.N. Labrenz and S.R. Sharpe, Phys. Rev. D **54** (1996) 4595.
- [29] B. Crouch, D.B. Leinweber, A.W. Thomas and R.D. Young, in preparation.